International Astronautical Congress (IAC 2021), Dubai, United Arab Emirates, 25-29 October 2021.

IAC-21-D2.3.1 (x66011)

Advanced European Re-Entry System Based on Inflatable Heat Shields EFESTO project overview: system and mission design and technology roadmap

F. Trovarelli [a], G. Guidotti[f]*, G. Medici[a], T. Schleutker[b], I. Dietlein[c], G. Gambacciani[d], G. Governale[e], J.-L. Verant[g], Y. Dauvois[g], Y. Prevereaud[g]

[a] *DEIMOS Space S.L.U., Tres Cantos, Spain*
[b] *Deutsches Zentrum für Luft- Und Raumfahrt e.V. (DLR), Köln, Germany*
[c] *Deutsches Zentrum für Luft- Und Raumfahrt e.V. (DLR), Bremen, Germany*
[d] *AVIOSPACE SRL, Torino, Italy*
[e] *Department of Mechanical and Aerospace Engineering, Politecnico di Torino, Turin – Italy*
[f] *Centro Italiano Ricerche Aerospaziali (CIRA), Capua – Caserta, Italy*
[g] *Office National d'Etudes et de Recherches Aerospatiales (ONERA), Toulouse, France*
* Corresponding Author: giuseppe.guidotti@deimos-space.com

Abstract

European Union H2020 EFESTO project is coordinated by DEIMOS Space with the end goals of improving the European TRL of Inflatable Heat Shields for re-entry vehicles from 3 to 4/5 and pave the way to In-Orbit Demonstration that can further raise the TRL to 6. This paper presents the project objectives and provides a general overview of the latest advancements, promoting the relevance of the EFESTO know-how in the frame of a European re-entry technology roadmap. The system, aerodynamic and mission design of two Hypersonic Inflatable Aerodynamic Decelerator use case scenarios, the AVUM VEGA stage recovery and a high-mass Mars exploration EDL mission, have been selected for deriving requirements and constraints to be injected in the EFESTO ground testing phase. The focus of this phase was on the aerothermal verification of the Flexible-Thermal Protection System in the DLR Arcjet facility and the analysis of the mechanical properties of the Inflatable Structure exploiting a manufactured 1:2 demonstrator, both representing key aspects of this peculiar and innovative technology.

Keywords: Reusability, Mars Exploration, EDL, Flexible-TPS, Inflatable Structure, Aerodynamic Decelerators.

1. Introduction

The European Union H2020 EFESTO project is coordinated by DEIMOS Space with the end goals of improving the European TRL of Inflatable Heat Shields for re-entry vehicles from 3 to 4/5 and paving the way to further improvements to be implemented in a possible future IOD to achieve TRL 6, eventually in agreement with ongoing and future European efforts in this context [1]. The project includes design and ground test activities, covering the key subsystems of inflatable structure and Flexible-Thermal Protection System (F-TPS) that compose a Hypersonic Inflatable Aerodynamic Decelerator (HIAD).

This paper provides an overview of the project, the outcomes of the detailed design of atmospheric entry mission scenarios and an overview of the technology roadmap together with the aerothermal and structural test campaigns, consolidating and extending the results already presented in [2]. In particular, the recovery of reusable small launcher upper stages and a high-mass Mars robotic exploration EDL mission have been selected as testbeds for the characterization of the performance that HIAD systems shall guarantee.

For the Earth Application, the recovery of the AVUM VEGA upper stage has been chosen as baseline case study. The current mission layout consists of a deorbit from Polar Orbit followed by a controlled entry phase. Atmospheric deceleration is achieved using a 4.5m diameter class HIAD followed by a parachute descent phase. Finally, a parafoil shall enable Mid-Air-Retrieval (MAR) of the entry vehicle with a helicopter. The Mars robotic exploration mission design resulted in a 9m diameter HIAD class, combined with Supersonic Retro-Propulsion (SRP) for safely landing the 2.5 tons payload at MOLA +3km target altitude.

The AVUM recovery entry mission analysis confirmed the HIAD as an appealing, performing and robust solution for the purpose of safely returning this VEGA upper stage to a targeted recovery area. For the Mars application mission analysis showed that, compared to state-of-the-art technology, the implementation of the HIAD efficiently provides larger drag during the entry phase, thus allowing to increase both landed mass and MOLA altitude at which a soft landing is possible.

2. VEGA AVUM stage recovery mission EDL

After injecting its payload into the target orbit, the AVUM VEGA upper stage performs a deorbiting manoeuvre and, not being protected by any TPS, it burns up in the Earth's atmosphere, eventually demising in a safe area for ground population. In any case, this valuable hardware is currently lost at the end of each VEGA launch.

The first key aspect considered in EFESTO to make this stage reusable is the need to protect the AVUM with a HIAD from the harsh entry environment. A feasible trajectory shall comply with a set of applicable constraints and in particular those limiting the thermo-mechanical loads during entry.

The second aspect considered is the possibility of recovering the AVUM at the end of the re-entry flight with limited operational effort. The launch costs cut by reusing this hardware shall in fact outweigh the cost of recovery. A preliminary business case analysis has shown that the latter should not exceed the 10% of the value of the recovered hardware. For the AVUM case the most cost-efficient option consists of exploiting helicopters for MAR operations.

The reference EFESTO Earth full mission layout in Fig. 1 starts with the VEGA launch and injection of the payload into the target orbit (1), followed by the deorbiting manoeuvre and the separation of the payload adapter (2). At this point the HIAD is inflated and a controlled lifting entry phase starts (3). The Centre of Gravity (CoG) of the HIAD is offsetted so that the vehicle is able to generate the necessary lift to be used for steering the flight trajectory. The entry phase ends at around Mach 1.6 when the pilot chute is ejected to extract a drogue parachute that further decelerates the payload (4). A parafoil deployed at low subsonic conditions guides the vehicle to the targeted MAR area (5). The final step is the necessary refurbishment of the recovered stage (6) to prepare it for the following flight.

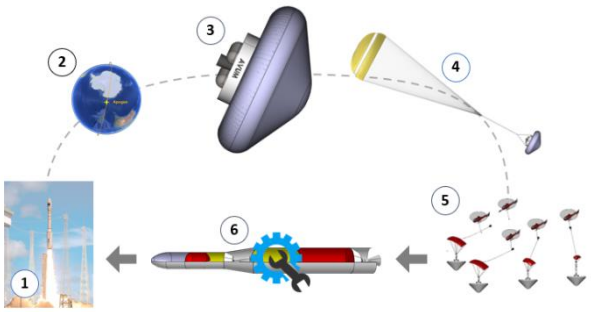

Fig. 1. VEGA AVUM recovery CONOPS.

2.1 Entry vehicle system configuration

The HIAD shield shall enable the AVUM recovery without modifying the existing VEGA launcher subsystems distribution as defined in the User Manual [3]. The solution envisioned consists of storing it within the available volume under the VESPA.

The resulting system configuration is given in Fig. 2. The inflatable structure consists of two integrated volumes pressurized using a cold gas generator. The annular torus has a tear-shaped cross section and an outer diameter of 4.8m while the secondary conical volume covers the lateral surface area of the cone, that has a total height of 2.1m and an opening angle of 120°. The spherical rigid TPS nose measures 1.3m in radius. The resulting reference surface of the vehicle in entry configuration is around 18 m².

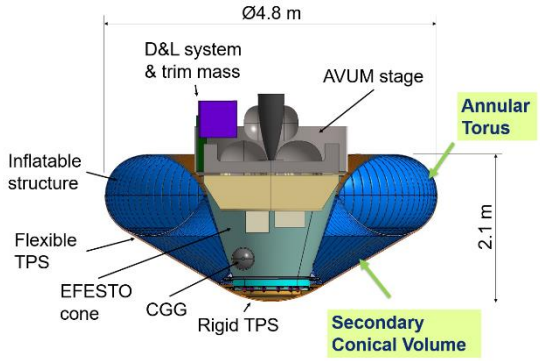

Fig. 2: Earth scenario HIAD entry vehicle.

2.2 Entry vehicle aerothermodynamics

The aerodynamic coefficients of the vehicle have been defined for a lifting entry trajectory flown at a nominal Angle of Attack (AoA) of -15°. The initial AErodynamic DataBase (AEDB) was generated for selected trajectory points using the engineering code ARES, based on the FAST aerodynamics and aerothermodynamics solver [4,5], that guarantees minimal computational effort. The computation was later refined taking advantage of CEDRE (Calcul d'Écoulements Diphasiques Réactifs pour l'Énergétique) Computational Fluid Dynamics (CFD) tool [6] which provides an estimation of the coefficients for a wider range of Mach numbers (2 to 25) and AoA (-30° to +30°).

Fig. 3 summarizes the values of the aerodynamic force coefficients generated by the vehicle flying at the nominal AoA as a function of the Mach number. It also shows the uncertainties due to discrepancies between the ARES and the CEDRE results and between the latter and flight data derived from the similar Apollo AS202 mission case.

It has to be noticed that the ARES solutions do not take into account turbulence and radiation heat transfer effects that might have a significant impact on the value of the wall heat flux, the latter depending on both re-entry conditions and vehicle size. In order to evaluate viscous and heat transfer contributions, CEDRE solver was used. In the computation a fully turbulent flow triggered at Mach 22.6 trajectory point, corresponding to maximum

stagnation heat load from preliminary trajectory propagation, has been assumed. The F-TPS is threated as a super-catalytic wall that provides the highest atomic recombination process model and best matches the expected properties of the F-TPS material. Finally, it was assumed radiative equilibrium with a material total emissivity of 0.8 to account for the radiative cooling mechanism. The radiative heat transfer process has been estimated as being not a predominant heat transfer mechanism for the specific mission conditions.

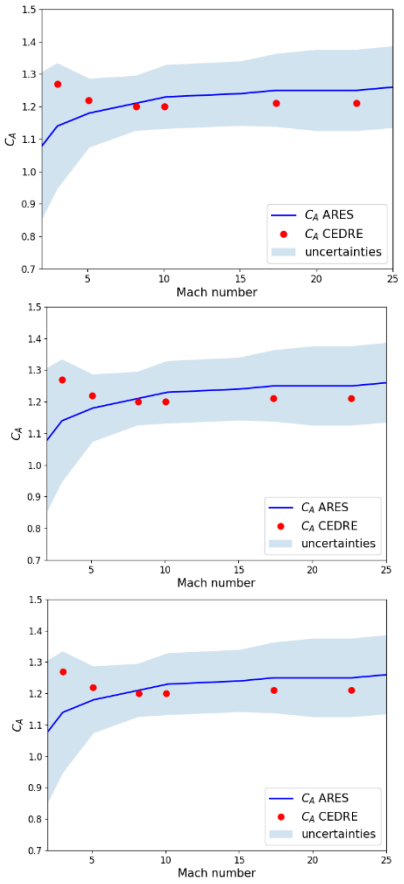

Fig. 3. Earth HIAD axial force, tangential force and moment aerodynamic coefficients.

Fig. 4 gives the temperature distribution obtained from the aerothermodynamic simulation under these assumptions on the Mars entry vehicle flying at Mach 22.6 and AoA -15°.

The simulation results indicated that the peak heating conditions are reached at the stagnation point. In here the heat flux equals 425 kW/m², while it varies from 230 kW/m² to 380 kW/m² on the windward surface of the cone and between 160 kW/m² and 400 kW/m² on its leeside. The analysis also confirmed stagnating flow, corresponding to extremely low heat flux values, in the AVUM payload rear zone of the vehicle.

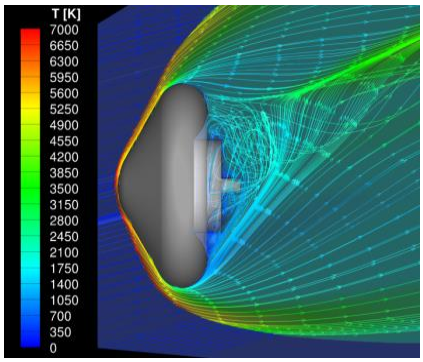

Fig. 4. Temperature distribution on the Earth HIAD flying at Mach 22.6 and AoA -15°.

2.3 EDL mission analysis

Fig. 5 shows the consolidated 2D Local Entry Corridor (LEC) that was defined for the vehicle described in the previous sections and assuming an Entry Interface Point (EIP) velocity of 7.6 km/s and parachute deployment at Mach 1.6. In this plot each curve is an isoline corresponding to either simple indicators, used in this case for relating the mission analysis with the thermal test campaign and the F-TPS design process, or active constraints not to be violated. The grey region contains the envelope, defined in terms of Ballistic Coefficient (BC) and flight-path-angle at EIP, that fulfils all imposed constraints. LEC is part of Deimos proprietary PETBOX atmospheric flight analysis tool [7].

The LEC analysis has shown that the entry corridor is limited by landing accuracy on the shallow side and by the maximum tolerable load factor and the maximum tolerable heat flux at the F-TPS cone for higher BC values on the steep side. For the reference vehicle layout, with an entry mass of 1096.61 kg corresponding to a BC of 46 kg/m², the entry corridor is 1.8º wide, ranging from -3.79º to -1.97º.

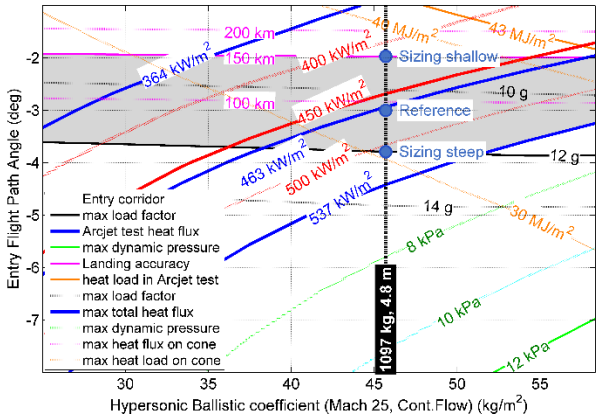

Fig. 5. Earth entry mission scenario 2D LEC.

The poor landing accuracy achieved by a pure ballistic HIAD entry, not complying with the recovery

mission requirements due to a wide range of dispersions at EIP, suggested the need for a controlled lifting re-entry. As already mentioned, the offsetting of the CoG allowed to obtain a trim AoA, ranging between -10º and -20º, so that the HIAD can generate lift. The resulting range capability can be used for compensating dispersions by controlling the bank angle during entry flight.

Fig. 6 demonstrates that for a -15º AoA trim angle a theoretical range capability between 300 and 400 km, corresponding to a compensation of about 150 to 200 km in the EIP position error, can be achieved.

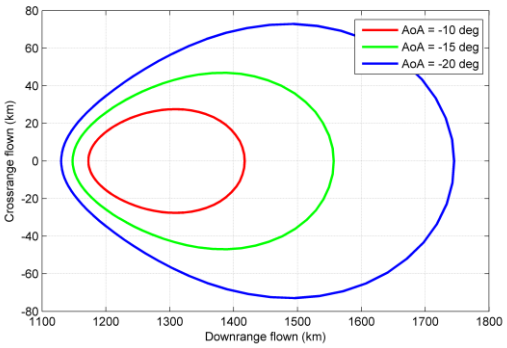

Fig. 6. Range capability as a function of trim AoA.

The results of the Monte Carlo campaign in Fig. 7 further confirmed that the chosen F-TPS sizing heat flux and aerothermal Arcjet test conditions are in line with the expected variability of atmospheric conditions during flight and perturbations in system mass and aerodynamic properties. Also, the same analysis demonstrated the compatibility of the achievable position accuracy at the end of the descent phase with the approximate 200km radius of the MAR area.

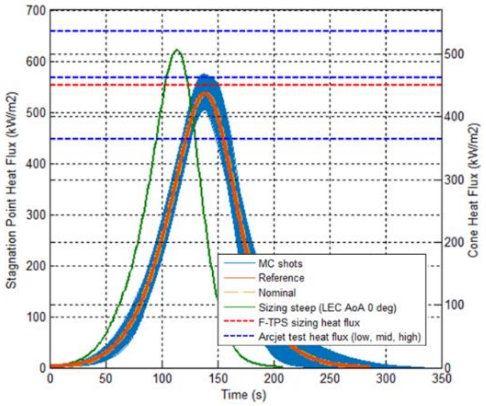

Fig. 7. Earth entry mission scenario Monte Carlo heat flux verification.

3. Mars robotic exploration EDL mission

The selected high-mass Mars exploration robotic baseline EDL mission is compatible with a launch in the 2030-2040 timeframe. Following an interplanetary transfer, the vehicle will perform a direct entry at hyperbolic arrival velocity in the Mars atmosphere. As depicted in Fig. 8, the first events consist of the cruise stage separation (1) followed by the separation of the bag protecting the stowed HIAD (2). After it gets inflated (3), the hypersonic re-entry phase starts. The HIAD provides aerodynamic deceleration until, after front shield ejection (4), it gets released (5). Touchdown speed is achieved using SRP down to ground (6), and finally a Skycrane-like system lowers the payload down to the surface (7).

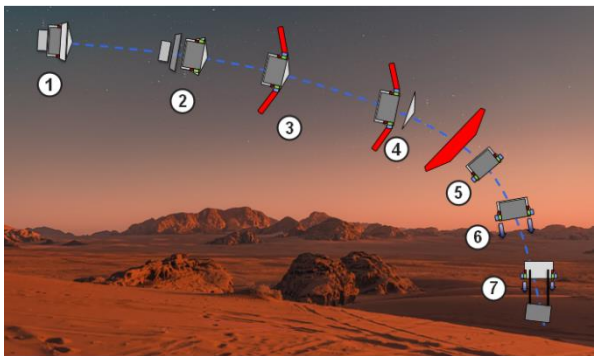

Fig. 8. Mars HIAD robotic EDL mission CONOPS.

3.1 System synthesis

The EFESTO Mars entry vehicle given in Fig. 9 houses a 2.5t scientific payload in a 2.8m x 2.5m envelope. The carrier frame in blue is equipped with the supersonic SRP system consisting of the fuel and helium tanks, avionics and the Skycrane-like equipment used to lower the scientific payload to the Mars surface. The SRP is a ring of multiple monopropellant Aerojet Rocketdyne MR-80B3100 thrusters that can be activated at Mach 2.3 and used down to hovering [8], where the touchdown manoeuvre is performed. The thrusters could additionally be used for compensating any CoG displacement or other perturbances during part of the EDL flight.

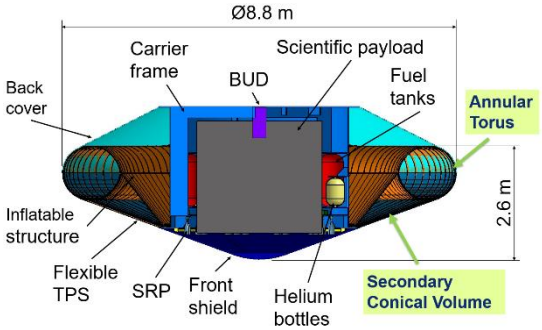

Fig. 9. Mars scenario HIAD entry vehicle.

The basic architecture of the HIAD is similar to that designed for the AVUM recovery on Earth. It features an annular torus defining an outer diameter of the inflated cone of 8.8m and a secondary conical volume. With a

total height of 2.6m, the opening angle of the cone measures 140°. The nose radius is 1.75m. The resulting reference surface of the vehicle in entry configuration in the order of 60m².

The interface between the HIAD and the rigid nose is integrated in the carrier frame. The HIAD is assumed to be pressurized using helium, already required for the pressurization of the fuel tanks. Alongside the rigid nose, heat protection is ensured by a properly dimensioned F-TPS and a flexible back cover complemented by an MLI layer on the back surface of the carrier frame.

3.2 Aerothermodynamics

As for the Earth mission, also for the Mars case the AEDB was preliminarily estimated at specific points of the reference ballistic entry trajectory using the ARES tool and later validated and extended with a dedicated CEDRE CFD campaign. Fig. 10 gives the estimated axial aerodynamic force coefficient of the entry vehicle, the others being null at AoA 0°.

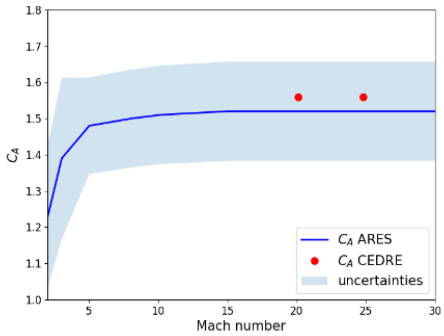

Fig. 10. Mars HIAD axial aerodynamic force coefficient.

The numerical procedure to assess heating loads on the Mars HIAD entry vehicle, follows the same analysis path already described for the Earth mission. In particular, the assumptions already discussed regarding the super-catalytic wall, the radiative cooling and the shock layer radiative heat transfer process in combination with turbulence effect, still hold. The atmosphere, however, is assumed to be 100% CO_2. Fig. 11 gives the temperature distribution obtained from the aerothermodynamic simulation under these assumptions for the Mars entry vehicle flying at Mach 25 and AoA 0°.

The results of the CFD campaign show that the local conditions of the Mars entry trajectory, in combination with the large size of the vehicle, trigger a laminar-to-turbulent transition mechanism at around the junction between the sphere and the cone. The result is that the heat flux increases along the frontshield with respect to the stagnation point conditions so that, contrarily to the Earth mission case, the peak heating conditions are experienced on the surface of the HIAD cone.

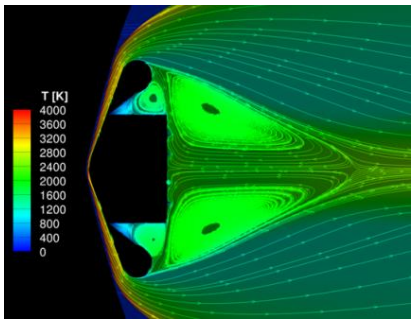

Fig. 11. Temperature distribution on the Mars HIAD flying at Mach 25 and AoA 0°.

In particular, the heat flux at the stagnation point is equal to 289 kW/m², while on the cone it reaches 458 kW/m². On the back shield, as expected, the stagnating flux guarantees low heat flux between 7 kW/m² and 11 kW/m². Finally, due to high temperature CO_2/CO and N_2 atmospheric mixture species, infrared radiative over-heating is a Martian entry environment specificity to be accounted for. The calculation of this contribution resulted in additional 30 kW/m² experienced at the front-shield.

3.3 Mission analysis

Fig. 12 shows the consolidated LEC that was defined for the vehicle described above, assuming an EIP velocity of 6 km/s and HIAD release at Mach 2.3. For the Mars EDL mission, the entry corridor is limited by the landing accuracy limit on the shallow size and by the maximum tolerable heat flux at the F-TPS cone on the steep side. The compliance with the landing accuracy can already be guaranteed by a ballistic entry and no controlled lifting re-entry is necessary.

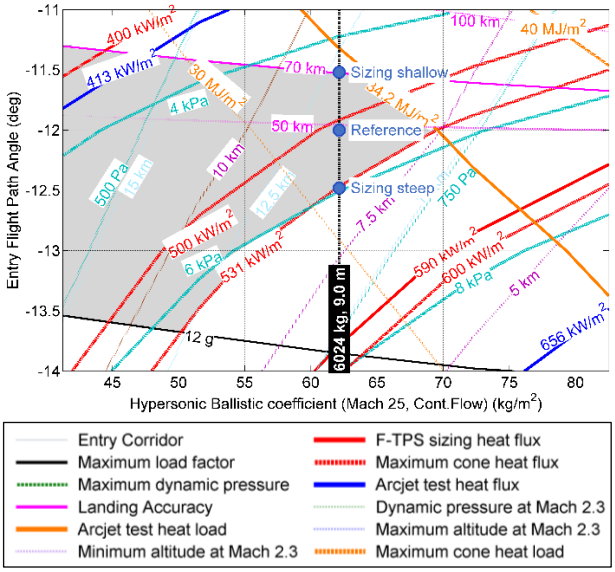

Fig. 12. Mars entry mission scenario 2D LEC.

For the reference vehicle layout, with an entry mass of 6024kg corresponding to a BC of 62 kg/m², the entry corridor is 1º wide, ranging from -12.5º to -11.5º, suggesting a much steeper trajectory with respect to the Earth case, as expected as a result of the lower atmospheric density.

The additional 30 kW/m² due to the radiative component raise the expected maximum heat flux on the HIAD cone to 561 kW/m². This value, however, is still in line with the F-TPS sizing heat flux of 590 kW/m². The results of the Monte Carlo campaign in Fig. 13 further confirm that the chosen F-TPS sizing heat flux and aerothermal Arcjet test conditions are in line with the expected peak heat flux variability caused by variable atmospheric conditions during flight and perturbations in system mass and aerodynamic properties.

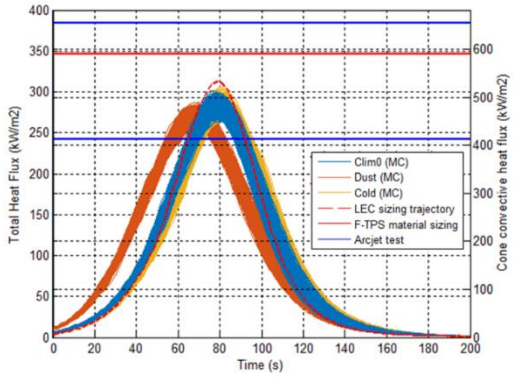

Fig. 13. Mars entry mission scenario Monte Carlo heat flux verification.

The Monte Carlo campaign additionally proved that the SRP system is able to handle the perturbations and always achieves a soft landing within the required 50km landing accuracy requirement. The performance of the coupled HIAD and SRP deceleration in terms of fuel efficiency, however, revealed significant sensitivity to the atmospheric conditions encountered during the EDL flight.

The high versatility of the SRP system could theoretically allow to tune the EDL flight schedule, and in particular the location of the HIAD-SRP switch, with the objective of optimizing not only the mass that can be safely delivered but, eventually, also the MOLA altitude of the landing site. The sensitivity analysis that was carried out showed that anticipating the HIAD-SRP switch could make it possible to land a still relevant mass at higher MOLA elevation, while instead diving deeper with the HIAD into the atmosphere could significantly increase the landed mass. The former scenario would need an SRP system capable of operating at Mach larger than 2.3, while the latter would require that the vehicle in entry configuration, i.e., with the inflated HIAD, is stable at Mach numbers lower than 2, which is difficult to achieve for a typical Mars hypersonic entry vehicle shape.

4. EFESTO contribution to HIAD TRL increase

The preliminary and detailed design loops were followed by a ground effort aimed at investigating two key aspects of HIAD technology and raise the European TRL from 3 to 4/5. In particular, an extended aerothermal testing campaign was carried out for different F-TPS layups options and the mechanical properties of the inflatable structure where characterised using a relevant manufactured demonstrator. The details of these tests campaign are reported below.

4.1 Arcjet test campaign overview

The F-TPS is a foldable multi-layer structure consisting of an outer layer exposed to the external entry environment that has to withstand the highest temperature. It covers the inner layers that are meant to preventing the diffusion of heat to the internal structures and the payload. Within the EFESTO project several layups combination where designed and simulated, in agreement with HIAD system requirements. After a final screening, the three most promising F-TPS solutions, two for the Mars case and one for Earth, were subjected to thermal characterization tests in DLR's arc-heated facilities LBK, which allows comparative testing on sample basis at mission relevant conditions.

The LBK facilities consist of the two individual test legs, L2K and L3K. Both are particularly suited for thermal characterization and qualification of TPS materials and structures for atmospheric entry. The facilities allow for long-duration tests at flight relevant enthalpy conditions and within a realistic thermochemical environment.

The L2K facility can be used for tests in Martian atmosphere by using a mixture of 97% CO_2 and 3% N_2 as working gas. For thermal testing, samples and models are placed in the homogeneous hypersonic free stream. A comprehensive description of the LBK facility is given by Gülhan et al. [9,10].

The test matrix included tests in two different configurations. The stagnation configuration is highlighted in Fig. 14. The setup is particularly useful for evaluating the principal capabilities of the F-TPS layups in a high-enthalpy environment. The conditions are defined by the gas atmosphere, the heat flux and the stagnation pressure. The corresponding sample holder was developed in a previous ESA study [11] and could be re-used with minor modifications. On its front surface, the holder provides an open diameter of 45mm for the F-TPS sample. The layup can consist of several different layers of fabrics, insulation and gas barriers with a total thickness of up to 30mm.

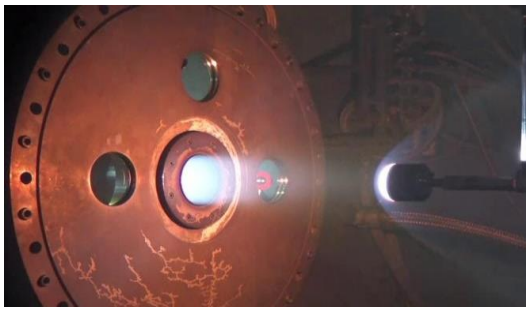

Fig. 14. Test environment for stagnation flow test.

The tangential flow configuration in Fig. 15 is more representative for the considered application as compared to the stagnation setup. This is because of the aerothermodynamic loading, that also includes shear stresses induced by the tangential flow. A new construction for the interior of the sample holder had to be designed and manufactured. The realized design allows exposure of a square area with 80mm side length to the tangential flow field. The holder keeps the outmost fabric layers under tension during the tests.

Fig. 15. Test environment for tangential flow test.

The test conditions were derived from the trajectory data of the respective applications in terms of heat flux, integral heat loads and stagnation pressure. During the tests campaign, main priority was given to the energetic parameters. Heat fluxes were varied up to the maximal entry flight heat flux predicted by the numerical simulations. The integral heat loads were set via the test duration. The heat load was also varied up to 150% of the predicted total heat load for demonstration purposes.

During all tests the F-TPS samples remained thermally stable. Post-test inspections did not indicate critical structural deficits, neither for the external fabric layers nor for the insulation layers. As illustrated by the photographs in Fig. 16, the exposed sample surfaces appeared uniformly heated in visual and infrared observations. Repetitive tests at identical test conditions showed a good reproducibility of the test results. All three F-TPS layups qualified for further consideration in the frame of the EFESTO applications.

Fig. 16. Sample appearance in stagnation test (left) and tangential flow test (right).

A second Arcjet test campaign is planned following the selection of the final layups, and will also include elements of the inflatable structure below the TPS, such as the F-TPS membrane.

4.2 IAD test campaign overview

The investigation of the mechanical behaviour of the inflatable structure as a sub-system was achieved through design, manufacturing and testing of a 2.4 m diameter demonstrator, scaled 1:2 with respect to the designed Earth case HIAD, in reference to already existing analogous test campaigns [12]. The demonstrator, pictured in Fig. 17 and photographed in Fig. 18, is a high-fidelity representation of the inflatable structure in terms of architecture, configuration, layout, and manufacturing solutions and additionally includes a fair-fidelity replica of the F-TPS and the outer mold-line of the AVUM stage.

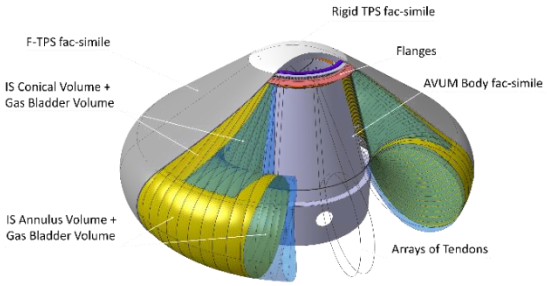

Fig. 17. HIAD demonstrator CAD model.

The focus of the testing campaign, executed in CIRA premises, was the verification of aspects related to stowing, folding, unfolding and inflation, followed by the verification of static strength under pressure pattern representative of re-entry conditions.

Fig. 18. HIAD demonstrator after inflation testing.

For the purpose of replicating the pressure load during re-entry, the implementation of a vacuum-pool with a non-porous membrane, pictured in Fig. 19 was selected. This test set up additionally required the design and manufacture of a dedicated test rig. Also, the demonstrator was equipped with load-cells and a video-footage of the system behaviour was recorded during test sessions to be used for later computational reconstruction.

Fig. 19. HIAD demonstrator under static load testing.

The test campaign was successful and allowed not only to achieve verification of the HIAD structural integrity but also to increase the knowledge of HIAD behaviour and support both modelling and numerical correlations.

5. EFESTO technology roadmap

The European advancements in the inflatable aerodynamic decelerators technology can enable future space missions, allowing new scientific and technological achievements. These include the possibility of heavier payloads landed at higher elevations, resulting in an expansion of the planetary exploration boundaries, or, by integrating the HIAD in the launcher vehicle, the ability to the recover some of its main components.

To reach such operational capabilities, the EFESTO project is carrying out the technology development of the F-TPS and the inflatable structure. The test campaigns described earlier are filling the gap between the current state of the art and the TRL for a future IOD mission which is foreseen by the EFESTO technology roadmap.

The roadmap in Fig. 20 is built on a technology context activity, assessing past, present, and future missions linked to the EFESTO activity by technology category. The current international efforts and space missions' goals are in line with the development of a technology capable of enlarging our landing and reusability capabilities.

Enabling the exploration of Mars in regions not yet accessible is of most scientific interest for the possible existence of life and to support future human exploration and colonization. The objective of enhancing reusability of Earth orbiting spacecraft by means of a potentially lightweight alternative to rigid decelerators is in line with the principle of affordability and sustainability, which represent key factors for the current space industry.

6. Conclusions

EFESTO project allowed to develop and improve the European know-how in the field of HIAD systems with respect to system design and engineering, key technology design manufacturing and testing. To complete the investigation exercise on these peculiar systems further effort shall be put in place in the future in agreement with the technology roadmap introduced.

The results presented demonstrate that HIAD systems represent an enabling technology for the next class of high-mass Mars exploration missions and this technology can be key in reducing the cost of access to space through upper stage reusability. The need for advancing the European TRL of this technology, which is the primary objective of the EFESTO project, is thus confirmed and the relevance of an IOD mission that will enhance the European know-how in the field, of which the EFESTO consortium represents the core, is reinforced.

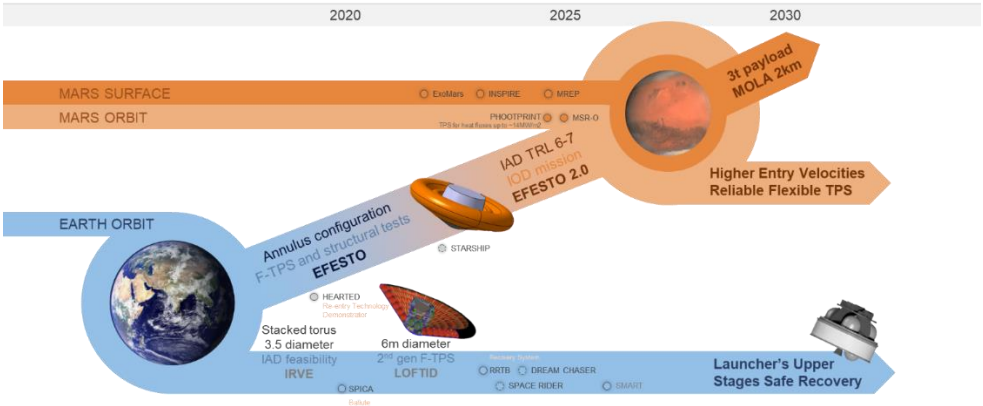

Fig. 20. EFESTO technology roadmap.

Acknowledgements

This project has received funding from the European Union Horizon 2020 research and innovation programme under grant agreement No 821801. More information available at:
https://cordis.europa.eu/project/id/821801

The EFESTO consortium acknowledges essential contributions from Thin Red Line Aerospace and ALI Scarl Italia concerning the IAD Demonstrator design, manufacturing, integration and testing processes.

References

[1] Dillman, R. A., DiNonno, J. M., Bodkin, R. J., and Hughes, S. J., "Planned Orbital Flight Test of a 6m HIAD," 15th International Planetary Probe Workshop, June 2018.

[2] Bonetti D., Dietlein I., Fedele A., Gambacciani G., Governale G., Prevereaud Y., "Advanced European Re-Entry System Based on Inflatable Heat Shields Detailed Design (EFESTO project)", 71th IAC, The CyberSpace Edition, October 2020.

[3] Vega User's Manual Issue 4 Revision 0, Arianespace, April 2014.

[4] Prévereaud, Y., "Contribution à la modélisation de la rentrée atmosphérique des débris spatiaux", Thèse de doctorat, Université de Toulouse (ISAE), Toulouse, France, Juin 2014.

[5] Annaloro, J., Galera, S., Kärräng, P., Prévereaud, Y., Vérant, J.-L., Spel, M., Van Hauwaert, P., Omaly, P., "Space debris atmospheric entry prediction with spacecraft-oriented tools", 7th European Conference on Space Debris, ESA/ESOC, Darmstadt, Germany, 2017.

[6] Refloch, A., Courbet, B., Murrone, A., Villedieu, P., Laurent, C., Gilbank, P., Troyes, J., Tessé, L., Chaineray, G., Dargaud, J., Quémerais, E., Vuillot, F., "CEDRE Software", ONERA Aerospace Lab Journal, 2011.

[7] Bonetti, D., Parigini, C., De Zaiacomo, G., Fuentes, I. P., Arnao, G. B., Riley, D., & Nogales, M. S. (2016). "PETbox: Flight qualified tools for atmospheric flight". 6th ICATT, Darmstadt, Germany, 2016.

[8] "In-Space Propulsion Data Sheets, Monopropellant and Bipropellant Engines," Aerojet Rocketdyne, September 1019.

[9] Gülhan, A., and Esser, B., "Arc-Heated Facilities as a Tool to Study Aerothermodynamic Problems of Reentry vehicles," Advanced Hypersonic Test Facilities, edited by F.K. Lu and D.E. Marren, Vol. 198, Progress in Astronautics and Aeronautics, AIAA, New York, 2002, pp. 375-403.

[10] Gülhan, A., Esser, B., Koch U., and Hannemann, K., "Mars Entry Simulation in the Arc heated Facility L2K," Proceedings of the 4th European Symposium on Aerothermodynamics for Space Vehicles, Capua, Italy, 2001, ESA-SP 487, pp. 665-671.

[11] Johnstone, E., Esser, B., Gülhan, A., Overend, S., Underwood, J., and Ferracina, L., "Investigating the Response of a Flexible TPS to a High Enthalpy Environment," Int. Conference on Flight Vehicles, Aerothermodynamics and Re-entry Missions & Engineering, Monopoli, Italy, October 2019.

[12] Swanson, G. T., A. M. Cassell, R. K. Johnson, S. J. Hughes, A. M. Calomino, and F. M. Cheatwood. "Structural strap tension measurements of a 6 meter hypersonic inflatable aerodynamic decelerator under static and dynamic loading." In AIAA aerodynamic decelerator system (ADS) conference, Daytona Beach, FL, pp. 25-28. 2013.

More information are available at: http://www.efesto-project.eu